ORIGINAL PAPER

Assessment of frost and heating penetration in compacted clay layers of landfill top covers in temperate climate

Giorgia Dalla Santa[1,2] · Simonetta Cola[1] · Antonio Galgaro[2,3]

Abstract

Compacted clay (CC) layers are commonly used as hydraulic barriers in landfills, thanks to their impervious capacity. However, mechanical and hydraulic properties of CC can be significantly affected by temperature variations due to the heat produced by waste degradation as well as to external air temperature and weathering. Previous experimental tests show that the most detrimental occurrence is the cyclic freezing–thawing (FT) that can increase the hydraulic conductivity of CC up to one order of magnitude. This paper aims at assessing the temperature distribution in a landfill multilayered top cover in several scenarios of temperature solicitations, in order to evaluate the depth of frost penetration. For this purpose, a 2D hydro-thermal coupled finite element model representing a case study landfill top cover has been developed; each constituting layer has been characterized by physical and thermal properties acquired through direct measurements on sampled materials in unfrozen and frozen conditions. The model provides a reliable time description of the isotherm distribution within the layered top cover in several temperature scenarios typical of a temperate climate, thus estimating the penetration of the frost front as well as of high temperatures.

Keywords Landfill top cover · Hydraulic conductivity · Frost front penetration · Compacted clay · Thermal conductivity

Introduction

In landfills, specific containing liners are engineered in order to isolate the contaminants from the surrounding environment and to minimize the escape of leachate and gases. The barriers used for the prevention of water and pollution migration are usually designed as layered systems, each layer serving a specific function, such as resistance to mechanical actions, drainage of internal fluids or gases, and barrier to fluid percolation and gas evaporation (for an overview of landfill design, see Victoria 2015; Rowe 2005). The latter function is typically provided by the compacted clay (CC) layers that close the landfill either at the bottom and at the top or laterally, thanks to their very low hydraulic conductivity reached after proper compaction. In addition, recent studies investigate how the mechanical and hydraulic performances of the CC barriers can be improved by means of amendments of recycled materials as tires or fly ash–sewage sludge mixes or water treatment sludges (Herrmann et al. 2009; Aziz et al. 2016; Chegenizadeh et al. 2018).

Depending on the type of waste that the landfill hosts, local regulations establish a threshold value for the required hydraulic conductivity (k) of the top and bottom landfill barriers. The European Community recommends a lower barrier with a maximum k equal to 10^{-9} m/s, or 10^{-7} m/s only in the case of inert waste, and an upper barrier including an "impermeable mineral layer" whenever the prevention of leachate formation is necessary (Annex 1 in Directive 1999/31/EC). Then, each member state is asked to incorporate these requirements into its local legislation. The Italian D. Lgs. n.36/2003 requires an impervious barrier with an effectiveness equivalent to a thickness of 1 m for the bottom and 0.5 m for the top layer with a maximum $k = 10^{-7}$ m/s. US regulations require the composite liners to contain a CC layer with a maximum hydraulic conductivity of 10^{-9} m/s at the bottom (CFR 40, I, 258-D) as well as at the top cover (CFR 40, I, 258-F).

✉ Giorgia Dalla Santa
  giorgia.dallasanta@unipd.it

1 Department of Civil, Environmental and Architectural Engineering - ICEA, Università Degli Studi Di Padova, Via Marzolo, 9, 35131 Padua, Italy

2 Department of Geosciences, Università Degli Studi Di Padova, Via Gradenigo, 6, 35131 Padua, Italy

3 Institute of Geosciences and Earth Resources, CNR Centro Nazionale Ricerche, Via Gradenigo, 6, 35131 Padua, Italy

Usually, the impervious performances of the CC layer are checked immediately after laying and compaction. The same performances must be maintained over the long term, in order to guarantee a lifelong proper effectiveness of the barrier system (Murray et al. 1996; Rowe 2005; Benson et al. 2011). Nevertheless, during the entire service life of the facility, the CC barriers are subjected to significant temperature variations mainly due to the following:

- Heat generated by the internal waste decomposition through physical, chemical, and microbiological processes occurring within the waste mass that varies over time and is temperature and oxygen dependent (Faitli et al. 2015)
- Weathering and external agents, such as air temperature fluctuations, solar radiation, and rainfall, that vary both daily and seasonally, according to the local climate (Hanson et al. 2009, 2013)

Heat generated by decomposition affects both the top and the bottom barriers, while weathering affects the top cover only. In particular, in temperate climates, cyclic subzero/overzero temperatures can establish freezing–thawing cycles in the cover, whereas during hot weather, high temperatures can induce drying processes. The concern is that temperature variations alter the mechanical and hydraulic properties of the CC layer.

A recent paper (Scaringi and Loche 2022) presents an extensive and comprehensive review of how temperature affects the engineering behavior of clayey soils in terms of compressibility, strength, and hydraulic conductivity in different conditions. Previous studies (Konrad 1989; Qi et al. 2008; Dalla Santa et al. 2016, 2019a) highlight that both freezing–thawing (FT) cycles and drying processes cause an irreversible change in the internal microstructure of CC barriers, resulting in the development of vertical fissures and cracks with reduced flow resistance that become preferential ways for permeation. In addition, the increase in hydraulic conductivity is shown to be greatest the first time the soil experiences FT or drying, as highlighted by Konrad (1989), Othman et al. (1994), Dalla Santa et al. (2016), and Sterpi (2015). Particularly, Benson and Othman (1993), Othman et al. (1994), and Benson et al. (2011) studied the CC hydraulic conductivity variations due to thermal solicitations by comparing the hydraulic conductivity of samples soon after the compaction procedure and after the exposition to heating/drying or freezing/thawing (FT) cycles, showing that the measured increase can be up to one order of magnitude. Aldaeef and Rayhani (2014) tested the effects of the combination of heating (up to 55 °C) and leachate exposures, while Albrecht and Benson (2001) analyzed the effects of wet-dry cycles on swelling and hydraulic conductivity

of CC. Finally, Othman et al. (1994), Benson and Othman (1993), and Sterpi (2015) studied the k variation caused by freeze–thaw cycles. As pointed out in a recent experimental study that compares the effects of FT cycles and wet/dry cycles (see Dalla Santa et al. 2020a), FT appears to be the more detrimental.

The observed effects mainly depend on the plasticity of the clay (Chamberlain and Gow 1979; Benson and Othman 1993; Othman et al. 1994), on compaction conditions such as compaction energy and water content (Sterpi 2015), and, finally, on the amplitude and duration of the imposed thermal solicitations (Aldaeef and Rayhani 2015; Albrecht and Benson 2001). Some authors observed that materials with higher plasticity (with PI ≥ 24% and high optimum water content w_{opt}) appear to be able to partially withstand the effects of thermal alterations, thus showing a slight recovery potential (Aldaeef and Rayhani 2015; Dalla Santa et al. 2020a). In general, however, the occurred degradation in terms of hydraulic conductivity is permanent.

Therefore, even if immediately after being laid a CC layer satisfies law requirements in terms of hydraulic conductivity, its impervious capability can deteriorate over time due to the effects of temperature oscillations. For this reason, as suggested in the previously cited research (Benson and Othman 1993; Albrecht and Benson 2001; Rowe 2005; Benson et al. 2011; Sterpi 2015), regulations prescribe protection of the CC layer from freezing and desiccation by spreading a 1-m-thick topsoil, which also enables leveling of the top surface and vegetation to take root. Nevertheless, in practice the laying of the top soil is sometimes postponed, due to various possible technical or financial issues (Moo-Young and Zimmie 1996; Chiemchaisri et al. 2010), incorrect construction procedures (Kim and Daniel 1992; Albrecht and Benson 2001) or following the formation of differential settlements in the cover due to the degradation process of wastes (Morris and Woods 1990; El-Fadel and Khoury 2000). Consequently, the CC layer may remain exposed to external agents and temperature fluctuations for some time (up to several months), covered by only a geosynthetic sheet.

Hydraulic conductivity alteration occurs only in the portion of the CC layer of the landfill top cover that is affected by freezing or drying, and the resulting impervious capacity of the entire barrier depends on the thickness of this portion, also in relation to the total thickness. An extensive experimental campaign on the changes in engineering properties affecting the cover barrier on site was performed by Benson and Othman (1993) and Benson et al. (2011). In particular, Benson and Othman (1993) performed a field test in South Eastern Michigan (USA) to monitor the penetration of the frozen fringe within the CC layer. In the test site, a test pad of instrumented CC was partially insulated and exposed to outside temperatures during the winter period in order

to measure the differential thermal behavior (between the insulated and uninsulated parts) during 10 FT cycles. In the uninsulated part, the observed frost penetration reached a depth of 0.5 m. In contrast, in the insulated portion of the test pad, no freezing occurred.

The hydraulic conductivity was measured both in field and in laboratory on specimen samples from the site. Although laboratory tests show that the hydraulic conductivity of specimens sampled within the zone of frost penetration was 50–300 times higher than before FT, no significant difference in hydraulic conductivity of the CC layer between the insulated and uninsulated portions of the test pad was registered on-site. The authors ascribed this effect to the large thickness of the test pad, equal to 1.5 m, given that in this case the portion subjected to frost penetration was so restrained that it could be considered irrelevant in terms of the overall impervious capacity of the entire barrier. This may not be the case when the top CC barrier has a limited thickness, such as the 0.5 m required in Italy.

Therefore, assessment of the temperature pattern and frost penetration within the cover is crucial in order to determine the consequent variation of hydraulic conductivity of the entire top cover and thus the deterioration of its effective impervious capacity over the long term. Temperature penetration within the CC layer mainly depends on the external and internal thermal solicitations (such as air temperature fluctuations and waste mass temperature) and on the characteristics of the top cover, such as its thickness and thermal properties of its composing layers.

Yeşiller et al. (2008) performed a long-term field investigation to determine temperature distribution and thermal gradients in covers of landfills located in four climatic regions of North America, ranging from cold temperate oceanic boreal conditions (Alaska) to warm-temperate subtropical semi-desert conditions (New Mexico), and hosting different waste ages. This allowed the researchers to study the influence of climate combined with the effects of the disposed waste age on the temperature within the waste mass itself and the cover. Field data were collected for more than 3 years by means of vertical and horizontal arrays of sensors placed within the temporary and the permanent cover systems and then compared with data acquired by control arrays inserted in the undisturbed ground nearby, thermally affected by the climate but not by the waste-produced heat.

Temperatures measured in covers varied seasonally according to air temperature, showing an amplitude decrement and a phase lag with depth. In addition, the internal temperature of the waste during disposal appeared to influence the thermal response of the cover over a brief period, owing to the ability of wastes to conduct and store heat. The long-term annual temperature cycle stasis onset in the cover is reached approximately 3 years after waste placement and does not depend on the its initial temperature (Yeşiller et al. 2008). The obtained results showed that seasonal air temperature fluctuations are predominant in controlling cover temperatures, while the presence of underlying wastes producing heat results in warmer temperatures and lower frost penetration in the cover, when comparing the temperature distribution within the cover to the one of the nearby subsoil. The field data were processed to produce predictive models and charts to obtain top cover temperatures and frost penetration depth starting from the local air temperature (Yeşiller et al. 2008). The proposed charts were elaborated by using constant thermal properties of the cover materials, although the thermal properties assume an important role in the thermal response of the top cover to external solicitations and in the consequent temperature evolution over time, given that thermal properties of a sediment vary with temperature, and more significantly in case of phase change.

This paper aims at assessing the evolution of the temperature distribution and frost penetration achieved in the top cover of a landfill subjected to a continental temperate climate, by means of a finite element model (FEM), where the thermal properties of the materials constituting the top cover have been derived from direct measurements on samples. The section of the landfill cover was modeled in 2D with the software FEFLOW released by DHI WASY, which can correctly analyze water and heat transport phenomena (Diersch 2005, 2014; DHI 2017a), and the cover's thermal behavior was analyzed in different scenarios of temperature solicitations.

The case study taken here as reference is the municipal solid waste landfill located in Torretta, near Rovigo, situated in Northern Italy's Po plain. Local weather data were compiled over several years in order to obtain significant temporal series. In addition, for proper definition of the model materials' thermal behavior, each layer constituting the top cover (drainage layer, CC barrier, and geotextiles) was sampled and tested to characterize its physical and thermal properties over a wide range of temperatures, frozen conditions included. The software then considered the changes in the material's thermal properties caused by the freezing/thawing phenomena by applying a proper plug-in.

The FEM model analyzes the temperature pattern evolution within the cover in different scenarios, under the combined effects of air temperature variations (with extreme values varying from 38 to -8 °C) together with the effects of the heat generated by the internal waste degradation (Yeşiller et al. 2008; Hanson et al. 2009). The final goal is to estimate the thickness of the cover that is in fact subjected to temperatures and estimate the deterioration of the top cover's impervious capacity in the considered scenarios.

Materials and methods

The layered structure of the tested cover

In the considered study case, the landfill top cover is analyzed in the worst possible situation, i.e., before placement of the protective top layer. It is therefore made up of the following layers, described from bottom to top: just over the waste sits a smoothing layer of loose sediment (tout venant) of an average thickness of 20 cm [layer 1]; this is covered by a 50-cm-thick drainage layer of gravel (with 16-/30-mm clasts) whose purpose is to collect biogas generated by waste biodegradation [layer 2]; finally, the top barrier constitutes a CC layer 50-cm thick [layer 3].

A sheet of high tenacity needle-punched polypropylene nonwoven geotextile (GTX-N) (300gr/m^2; 2.7-mm thickness) is placed between layers 1 and 2, mainly in order to separate the levels with different grain-size compositions while also allowing drainage and filtration. In addition, a woven polypropylene geotextile (TP060060W) (310 g/m^2) is inserted between layers 2 and 3, mainly in order to protect the CC barrier. The entire sequence is represented in Fig. 2a.

The main materials were sampled on-site and characterized in terms of granulometric and mineralogical composition. Figure 1 shows the grain size distributions, and Table 1 reports the granulometric data.

(A) Sample A was obtained from the gravel drainage layer (layer 2) and is made up of clasts with variable angular shapes; the carbonate clasts are widely predominant,

Table 1 Granulometric data obtained for the gravel constituting the drainage layer (A) and the silty clay used for the CC barrier (B) by means of sieve analysis and aerometry

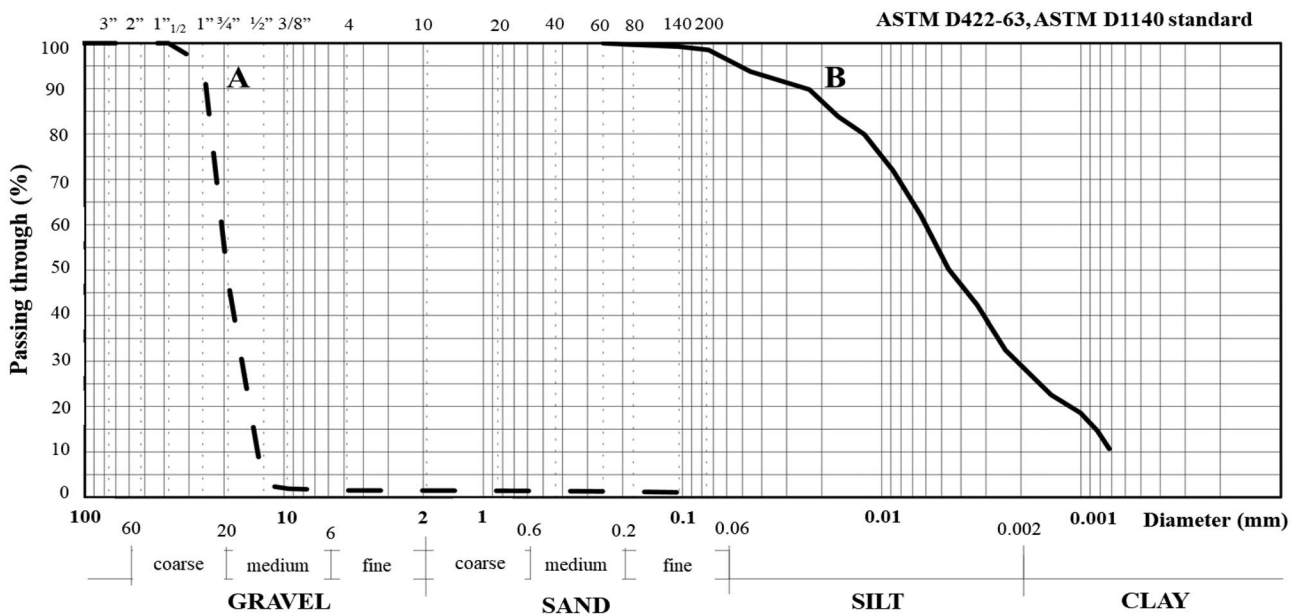| # Sieve (ASTM Standard)	Opening/corresponding particle diameter (mm)	Passing through [%]	
		Sample A	Sample B
1″ ½	38.1	100.00	100.00
1″	25.4	95.36	100.00
3/4″	19.1	47.51	100.00
1/2″	12.7	2.72	100.00
3/8″	9.52	1.89	100.00
4	4.76	1.51	100.00
10	2	1.48	100.00
20	0.84	1.43	100.00
40	0.42	1.37	100.00
60	0.25	1.30	100.00
80	0.177	1.22	99.67
140	0.105	1.09	99.26
200	0.074	1.00	98.51
	0.0457		93.74
	0.0325		91.76
	0.0231		89.79
	0.0166		83.85
	0.0122		79.90
	0.0088		71.99
	0.0064		62.10
	0.0046		50.23
	0.0033		42.32
	0.0024		32.43
	0.0014		22.55

Fig. 1 Particle size distributions of **A** the gravel constituting the biogas drainage layer and **B** the silty clay used for the CC barrier

with limited fractions of metamorphic and intrusive litho-types.

(B) Sample B was taken from the CC layer (layer 3) and is composed of high-plasticity inorganic silty clay, suitable for landfill linings as it is characterized by a liquid limit LL = 64 and a plasticity index PI = 32 (Murray et al. 1996; CFR 40, I, 258-F). Its mineralogical composition was evaluated by X-ray diffraction and validated by comparison to X-ray fluorescence chemical analysis, which detected phyllosilicates (69%, mainly illite and mica, with small components of vermiculite, chlorite, and kaolinite), dolomite (7%), quartz (18%), and feldspars (7%).

Thermal property measurements

The thermal properties of each material were measured by using the most appropriate measuring devices and methods.

(A) The thermal conductivity (TC) of the gravelly *drainage layer* (sample A) was measured by means of a guarded hot plate device, provided with a measuring plate of 0.8 m × 0.8 m and slightly modified for use with gravel samples, as described in Dalla Santa et al. (2017). The width of the measuring plates permitted testing samples with grains of large dimensions, thus resolving difficulties connected with the coarse size of the gravel clasts and the variability of their mineralogical composition (Jones 1988; Kömle et al. 2010).

The device used was a Taurus Instruments TLP 800, based on the steady-state method (the measuring characteristics are reported in Table 2), and the tests were performed at the IUAV FISTEC Laboratory (Environmental Technical Physics Laboratory of Venice University). The gravel sample was inserted into a tailor-made box (0.5 m x 0.5 m x 0.06 m) to be placed between the hot and the cold plates and was subjected to a temperature difference of 5°C, which is maintained constant during the whole test. The TC value was then obtained from the measured thermal resistance, the sample thickness, and the imposed temperature difference, subtracting the thermal resistance of the box. In order to consider the influence of water content, the measurements were conducted in three moisture conditions: dry (w=0%), partially saturated (w=23%), and almost saturated (w=96%). The test was first performed in dry conditions. Afterwards, measured amounts of water were gradually added to the sample by means of a nebulizer, until the voids were completely filled with water. This way, the testing method also allowed estimation of the gravel porosity.

(B) For the *silty-clay sediment* (sample B), the measurements were conducted with ISOMET2114 Thermal Properties Analyzer manufactured by Applied Precision s.r.o., a portable hand-held measuring device working on the basis of the transient heat transfer method (measuring range and accuracy are reported in Table 2). It analyses the material's thermal response to a known heat flow impulse applied to the tested material by an electrical resistor inserted into the sensor, directly in contact with the specimen. The instrument directly supplies the thermal conductivity and diffusivity, this way providing an indirect measurement of the volumetric heat capacity.

Given that TC of a sediment changes according to temperature variations (Farouki 1981; Nikolaev et al. 2013; Tarnawski et al. 2000), sample B was tested over a wide range of temperature, also in frozen conditions (from −18 up to +50°C). The specimens were prepared at a water content equal to 1.2 PL ca (porosity equal to 0.6); during the temperature changes and during the measurements, they were kept covered by a plastic bag in order to minimize the water losses.

(C) ISOMET2114 Thermal Properties Analyzer was also used to measure the thermal properties of the two *geotextiles*. Despite being extremely thin, their thermal properties affect the heat migration through the composite multilayered cover. Previous studies (Singh

Table 2 Characteristics of Taurus Instruments TLP 800 and of ISOMET 2114 Thermal Properties Analyser manufactured by APPLIED PRECISION s.r.o. (see Applied Precision user's guide 2013) (Slovakia)

Taurus Instruments TLP 800

Measured parameter	Value range	Accuracy
Thermal conductivity	0.005–2.0 Wm^{-1} K^{-1}	2.5%
ISOMET 2114 Thermal Properties Analyser		
Measured parameter	**Value range**	**Accuracy**
Thermal conductivity	0.015–0.70 Wm^{-1} K^{-1}	5% reading $+0.001$ Wm^{-1} K^{-1}
	0.70–6.0 Wm^{-1} K^{-1}	10% reading
Volume heat capacity	$4*10^4$–$3*10^6$ Jm^{-3} K^{-1}	15% reading $+1*10^3$ Jm^{-3} K^{-1}
Temperature	-20–70 °C	± 1 °C

Fig. 2 **a** Model domain. **b** Detail of the mesh refinement corresponding to the geotextile layers.
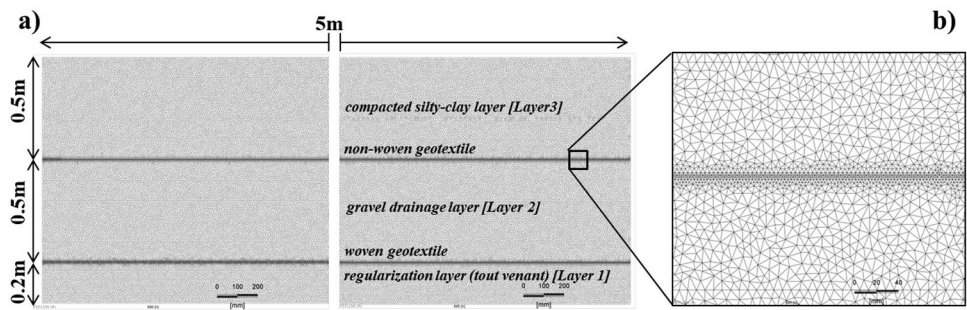
and Bouazza 2013) revealed that in geotextiles, the TC varies depending on water content, time of immersion in water, and surface treatment. The higher the water content and longer the time of water immersion, the higher the thermal conductivity. Therefore, in order to obtain representative values for the in-site conditions, the measurements were performed on geotextiles in both dry and saturated conditions (after 3 days of immersion in water).

Modeling investigations

The finite element modeling analysis was carried out using the FEFLOW (*Finite Element subsurface FLOW and transport simulation system*) software produced by DHI – WASY. FEFLOW can simulate coupled heat and mass transfer in soils by simultaneously integrating state equations describing the groundwater flow and heat transfer in porous media (DHI 2017a; Diersch 2005, 2014). It has a very wide range of applicability (see, for example, Casasso and Sethi 2015; Cultrera et al. 2018; Perego et al. 2020; Galgaro et al. 2020). Given the importance of considering the phase change processes within the model (Dalla Santa et al. 2019b), a recently released plug-in named PiFreeze has been activated (DHI 2017b). The objective of this explicitly developed plug-in is to correctly consider the thermal properties' variation due to the phase changes related to freezing processes. The theoretical background and the operative procedures implemented in the plug-in are reported in the FEFLOW PiFreeze User Guide (DHI 2017b).

Figure 2 represents the implemented model domain and the associated mesh. The model domain represents a 2D section of the landfill top cover: it is a 5-m-long and 1.212-m-wide

rectangle, subdivided into three main horizontal layers (Fig. 2a). The succession from bottom to top is therefore 200 mm of regularization layer, 500 mm of gravel (drainage layer), and 500 mm of compacted silty clay (impervious barrier). As on site, two 6-mm-thick geotextiles separate the main layers. The mesh of triangular elements was appropriately refined near the geotextile layers (see Fig. 2b) in order to support the computational resolution process resulting from abrupt changes in the material's physics and thermal features.

The materials' physical and thermal properties were defined by using the results obtained from the experimental tests conducted on samples explicitly, as presented and discussed in paragraph 3.1.

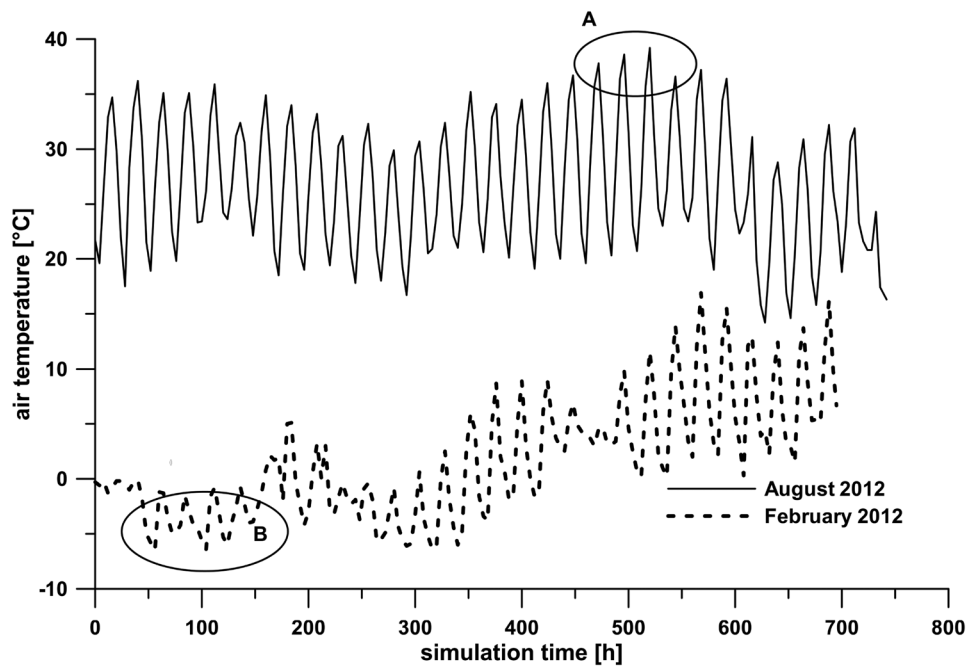The following thermal boundary conditions were assigned:

- At the upper boundary of the mesh, the hourly air temperature recorded by the Environmental Regional Agency (ARPAV) at the closest climatic station of Castelnovo Bariano (Rovigo province) from 2006 to 2015. Within this period, the highest and lowest temperatures, registered in August 2012 and February 2012, respectively (see Fig. 3), were assumed as the extreme thermal solicitations.
- At the lower boundary of the mesh, two temperature conditions were considered according to the degradation process of the underlying waste (as reported by Hanson et al. 2008, 2013): the temperature imposed by the high exothermic early stage, when a peak value of 70 °C could be reached, and the long-term temperature achieved in the waste mass, corresponding to about 30 °C.

Finally, the two "extreme" temperature boundary conditions on the upper and lower boundaries are combined in two different scenarios, in order to study the effects of the largest possible temperature solicitation, as shown in Table 3.

Table 3 Scenarios simulated with the analysis. The hourly temperature trends of August and February 2012 are represented in Fig. 3

Boundary condition	Scenario A	Scenario B
Air temperature (upper boundary)	Hourly temperature registered in **August 2012**	Hourly temperature registered in **February 2012**
Waste temperature (bottom boundary)	70 °C	30 °C

Fig. 3 Temporal series of air temperature measured in the local climate station in the months with the highest (August 2012) and lowest (February 2012) registered temperatures. Circles A and B highlight the maximum and minimum temperatures registered in the entire period 2006–2015, with air temperature extreme values of 38 °C and −8 °C, respectively

Results and discussion

Thermal properties of the materials

Thermal conductivity (TC) in gravels mainly depends on the porosity and on the granulometric and lithological composition of the gravel clasts, and it increases unevenly with water content (Nikolaev et al. 2013; Fricke et al. 1992). For this reason, the experimental measurements were performed on the gravel sample at several moisture contents starting from dry conditions and then adding known amounts of water. Figure 4 shows the TC data acquired for gravel sample (the tests were performed at room temperature, so the reference temperature is 20 °C).

The obtained results highlight the important contribution that water inside the pores provides to heat transport. The experimental values obtained from dry tests ($\lambda = 0.24$ Wm^{-1} K^{-1}) comply with the ones reported by Kömle et al.

The initial conditions of the temperature distribution within the entire model were defined by running a preliminary simulation which applied the air temperature measured during the previous 2 weeks to the upper boundary.

As for the hydraulic setting, the entire model domain was set as a variably saturated media, as indicated by Dogan and Motz (2005a, b). The initial water content condition was set at 0.2 for the compacted silty-clay layer and the underlying geotextile, while the regularization and drainage gravel layers were set at a moisture content of 0.2 (equal to about 0.3% of saturation).

(2010) for a similar carbonate gravel (87% calcite and 11% dolomite; clasts of 32–60 mm; porosity 0.51; $\lambda = 0.22$ Wm^{-1} K^{-1} ± 0.02). Despite the high TC of the constituent rocks (Schön 2015; Dalla Santa et al 2020b; Galgaro et al. 2020), the measured TC value in dry condition is rather low, possibly due to the high porosity connected to its poorly graded grain-size composition, i.e., there are very few intergranular contact points.

When water content is higher, a higher TC is measured. A sharp increase is observed passing from the dry situation to a water content of about 20–30%. The trends comply with the ones previously obtained for other gravels by using the same apparatus, as reported in Dalla Santa et al. (2017). This sharp increase can be ascribed to the fact that, starting from the dry sample, the first addition of water allows the formation of meniscus between the clasts (pendular and funicular
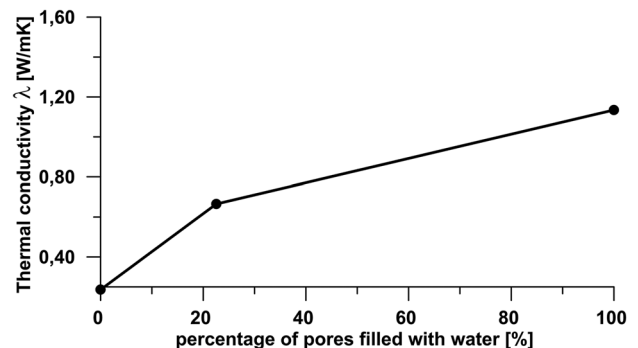
Fig. 4 Thermal conductivity obtained for the drainage layer from tests carried out with the Taurus Instruments TLP 800 (accuracy: 2.5%)

regimes), thus enlarging the connections between the solid components. As the water content further increases, water fills the gaps between the clasts (capillary regimes), thus allowing conductive heat transport inside the pores, in addition to the conductive heat transport inside the solid grains, as already observed by Nicolaev et al. (2013).

Owing to the large diameter of gravel clasts and large dimensions of the pores in the tested sample, the total heat transfer is produced by a conduction component inside the clasts themselves and inside the pore water, boosted by a convective component due to the local convective phenomena occurring in the wide pores and interconnections induced by the imposed thermal gradient. As a result, the adopted measuring method provides an "equivalent" TC value, which is influenced by both conduction and convective processes. It should be noted that convective phenomena occur locally, with limited mass transfer and at zero hydraulic gradient. As water content increases, the heat transfer capacity increases more gently, thus showing a nonlinear trend with water content; this can be attributed to the more homogeneous thermal condition achieved at higher water contents, leading to a lower convection contribution.

Figure 5 also reports the TC obtained for the two geotextiles tested at room temperature (20 °C) in dry and saturated conditions. The values are in accordance with those reported in literature for similar geosynthetics (Singh and Bouazza 2013).

Figure 5 also depicts the results obtained from the experimental tests carried out on the silty-clay samples at different temperatures, frozen conditions included. Figure 5a shows that while TC is almost constant at temperatures above zero ($\lambda_{SC} = 0.85–1$ Wm^{-1} K^{-1} with $2 < T < 50$ °C), a significant and abrupt change occurs when subzero temperature is reached and the sample freezes. Specifically, TC increased by about 80% (from 0.9 to 1.8 Wm^{-1} K^{-1}) from the reference value at 20 °C, reaching values up to 1.63–1.78 Wm^{-1} K^{-1}. During the phase transition, direct TC measurements are not reliable because of the unstable thermal behavior of the sample caused by latent heat release. For this reason, no values are reported around $T = 0$ °C. Figure 5b also shows the acquired volumetric heat capacity, which records the same abrupt changes. In this case, the volumetric heat capacity after freezing drops from 2 to 1.5 MJm^{-3} K^{-1} recording a variation of −25%.

As expected, the experimental findings highlight that transition to a frozen state brings about a sharp change owing to the partial filling of the voids with ice instead of water. As a result, conductive heat transport increases, while the thermal diffusivity decreases. In the frozen condition, thermal parameters change significantly owing to (I) ice filling the pores, which gives continuity to the porous medium, and (II) the different thermal properties of ice compared with those of water ($\lambda_{WATER} = 0.59$ Wm^{-1} K^{-1} and
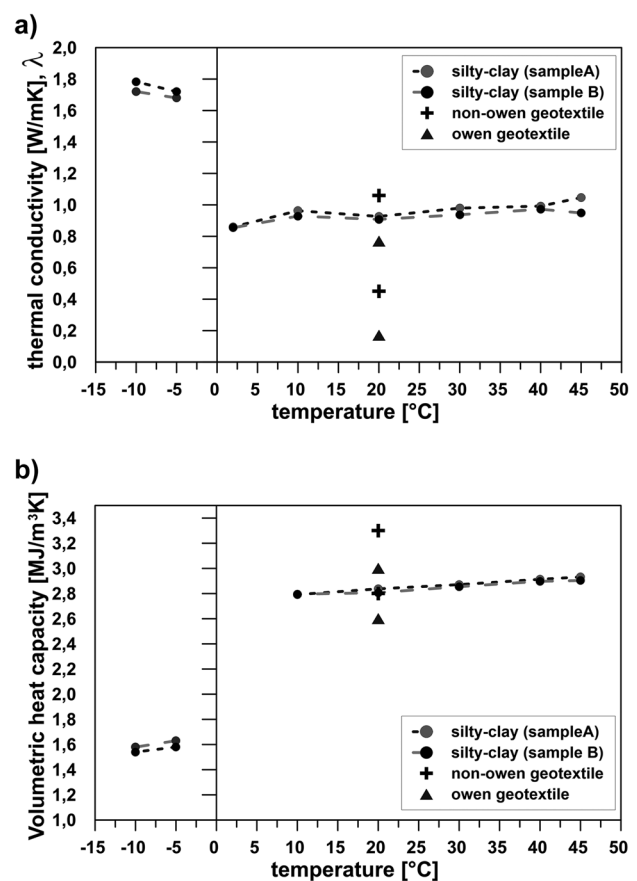

Fig. 5 Thermal properties obtained from measurements performed at different temperatures with ISOMET2114 on the two geotextiles in saturated and dry conditions and on the silty-clay samples; **a** thermal conductivity and **b** volumetric heat capacity

$rc_{pWATER} = 4.15$ MJm^{-3} K^{-1}, $\lambda_{ICE} = 2.32$ Wm^{-1} K^{-1} and $rc_{pICE} = 1.87$ MJm^{-3} K^{-1}). Consequently, frozen silty clay has a TC about 80% higher than and a heat capacity about 25% lower than non-frozen silty clay (considering that the reference values refer to 20 °C). This means that, on cold days, the frost front originating from subzero air temperatures, starting from the upper edge of the landfill top cover, can penetrate more rapidly and deeply into the interior of the compacted clayey liner, resulting in a larger portion of the CC barrier being subject to the alteration of the internal structure due to FT cycles. These experimental results demonstrate that, in the case of phase change, it is crucial to diversify the thermal behavior of the CC in the unfrozen and frozen state when assessing the numerical model as already highlighted in Dalla Santa et al. (2019b).

To properly analyze the thermal behavior of the landfill top cover, the data related to thermal properties acquired from the performed direct measurements were applied in the already described FE model to characterize the materials' properties.

Table 4 reports all the parameters assigned to the various materials in the model. To characterize the silty-clay barrier [layer 3], the TC and heat capacity were derived from the measured values, adjusted by taking into account the different porosity. For the sake of simplicity, the thermal conductivity acquired from the gravel sample was assumed for both the gravelly drainage layer [layer 2] and the regularization layer [layer 1]. Since the Taurus Instrument TLP 800 only provides the TC, the volumetric heat capacity of these layers was taken from the literature (Schön 2015) considering that the material is highly homogeneous and composed mainly of carbonate clasts.

In the two different scenarios analyzed (already defined in Table 3), different thermal properties were adopted to consider the effects of unfrozen/frozen conditions on soil depending on the imposed thermal solicitations. In scenario A, TC values in dry condition were assumed for all layers; in scenario B, values measured in saturated conditions were adopted for the CC layer, and the two geotextiles and values under wet conditions were adopted for gravel.

Modeling outputs–temperature distribution within the top cover

The model was run under the two scenarios already defined in Table 3, thus obtaining the temperature distribution along the entire section of the landfill top cover as a function of the thermal stress imposed as boundary conditions and of the materials' thermal properties.

In the FE model, a series of observation points were placed at increasing depth from the upper boundary of the model domain in order to monitor the local temperature evolution over time in both the CC layer (observation points 1 to 10) and in the drainage layer (11 and 12).

Figures 6 and 7 depict the temperature distributions in the landfill top cover section provided by the model in the two considered scenarios; Fig. 6a depicts the isotherm pattern obtained under the higher temperature stress (scenario A), while Fig. 6b, c depict the isotherms obtained under the lowest temperature stress, with the air temperature reaching the minimum value of −8 °C and thus leading to freezing (scenario B). The difference between these two patterns arises from the fact that the outputs in Fig. 6b are obtained considering the change in thermal properties due to the phase change, while those of Fig. 6c are obtained without considering the change in thermal properties.

In scenario A (Fig. 6a), it is evident that the more intense thermal stress generated by the degradation of the waste mass (70 °C) applied at the lower boundary induces a steep temperature gradient mainly constrained in the lower regularization layer, due to the very low TC of the woven geotextile (here considered in dry condition due to the high temperature achieved) and of the overlying gravel drainage layer, which is characterized by high porosity, and thus acts as a thermal insulator. For the same reason, a significant temperature gradient is established also in the upper CC layer under the air temperature imposed at the upper boundary: in this scenario, the CC barrier reached temperatures above 30 °C in its almost entire thickness, thus exposing the CC barrier to the risk of desiccation.

In contrast, in scenario B (Fig. 6b), the subzero thermal solicitation imposed by the air temperature at the upper boundary border causes the frost penetration within the CC barrier, which is characterized by a higher TC, as soon as the freezing conditions are reached. The temperature gradient affected the entire CC barrier and also developed in the drainage and regularization layer given the higher TC of the geotextile, here considered in wet conditions. Finally, the model output provides the estimated frost front penetration, here represented with the depth reached by $T = 0$ °C isotherm at the time of minimum air temperature solicitation (also indicated by the red line in Fig. 7). In the considered scenario, the frost penetration is equal to 17 cm, despite the fact that the heat originating from the degradation of the

Table 4 Material parameters adopted in the numerical model

Material	Thickness [mm]	Porosity [k-]	Hydraulic conductivity [ms⁻¹]	Thermal conductivity [Jm⁻¹ s⁻¹ K⁻¹]	Volumetric heat capacity [MJm⁻³ K⁻¹]
Compacted silty-clay layer	500	0.2	$1.03*10^{-8}$	1.17 (unfrozen) 1.45 (frozen)	1.47 (unfrozen) 1.05 (frozen)
Non-woven geotextile	6	0.7	$5*10^{-3}$	0.45 (dry) 1.1 (wet)	3.3 (dry) 2.8 (wet)
Gravel drainage layer	500	0.35	10^{-2}	0.24 (a)	1.8 (b)
Woven geotextile	6	0.7	$3*10^{-3}$	0.17 (dry) 0.8 (wet)	3 (dry) 2.6 (wet)
Regularization layer	200	0.3	10^{-3}	0.24 (a)	1.8 (b)

(a)Values acquired from the measurements performed at 20°C in dry conditions (Fig. 4)

(b)For the gravelly layers, the volumetric heat capacity has been deduced from literature (Schön 2015)
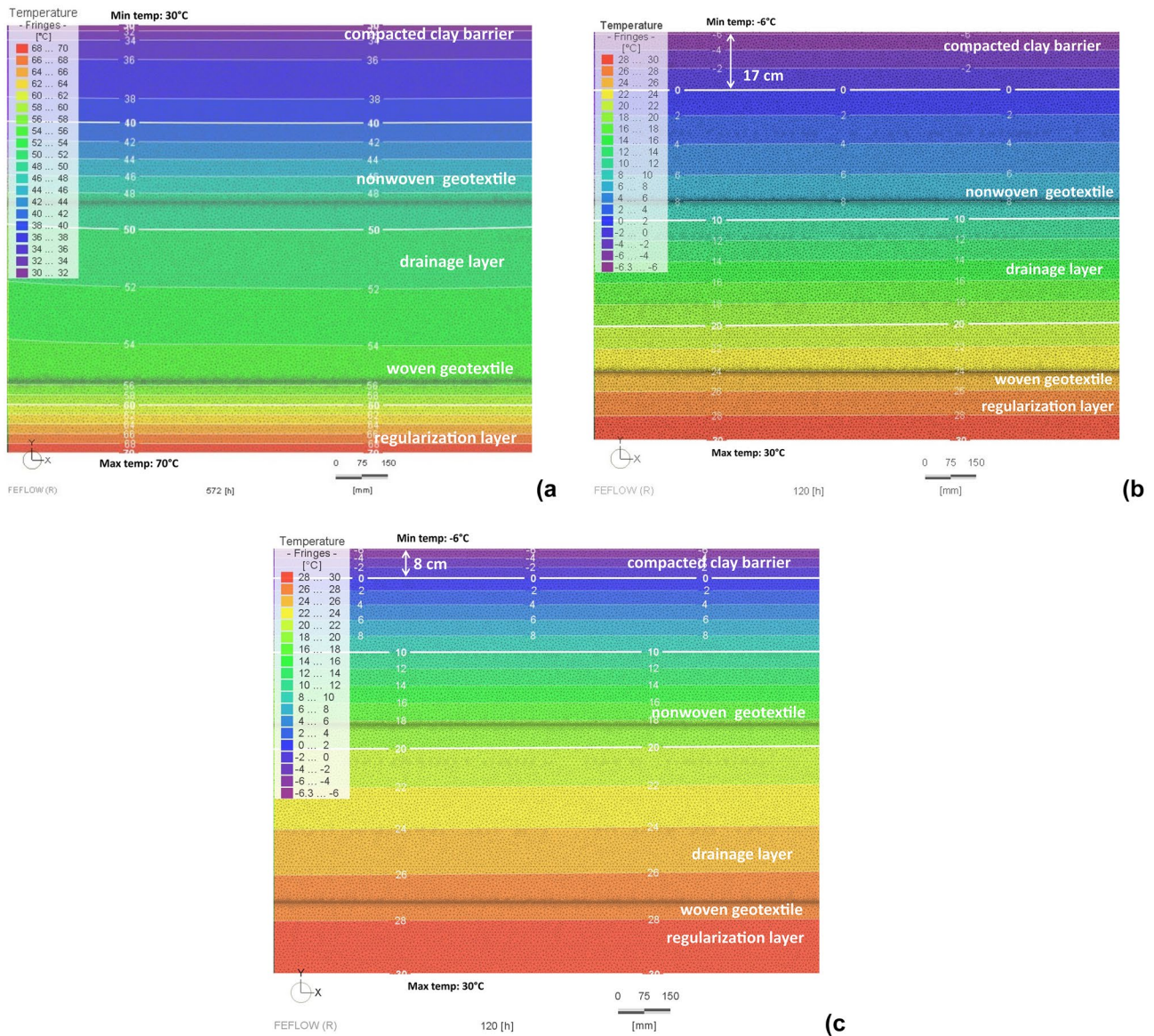
Fig. 6 Temperature distributions achieved in the landfill top cover as provided by the FE model in **a** scenario A, **b** scenario B considering the change in thermal properties induced by clay freezing, and **c** sce-nario B without considering the change in thermal properties induced by clay freezing. The temperature scales are adjusted to better represent the temperature patterns in the different scenarios

waste mass even in the long term can partially mitigate the effects of low air temperature, as previously observed by Yesiller et al. (2008). The obtained temperature distribution reported in Fig. 6b agrees with the values reported in literature as experimentally measured on site in similar climatic conditions (Benson and Othman 1995; Yesiller et al. 2008; Hanson et al. 2009).

The obtained results highlight the different thermal behaviors of the CC layer compared with those of the coarser layers. The CC layer is characterized by the following:

- Higher thermal conductivity (about 1 Wm^{-1} K^{-1} in unfrozen condition, which increases by about 80% in the frozen state) and lower heat capacity (about 2 MJm^{-3} K.$^{-1}$ in unfrozen condition, which decreases by about 20% in the frozen state)
- Saturation conditions, due to fact that the laying operations are performed at a slightly higher than optimal water content
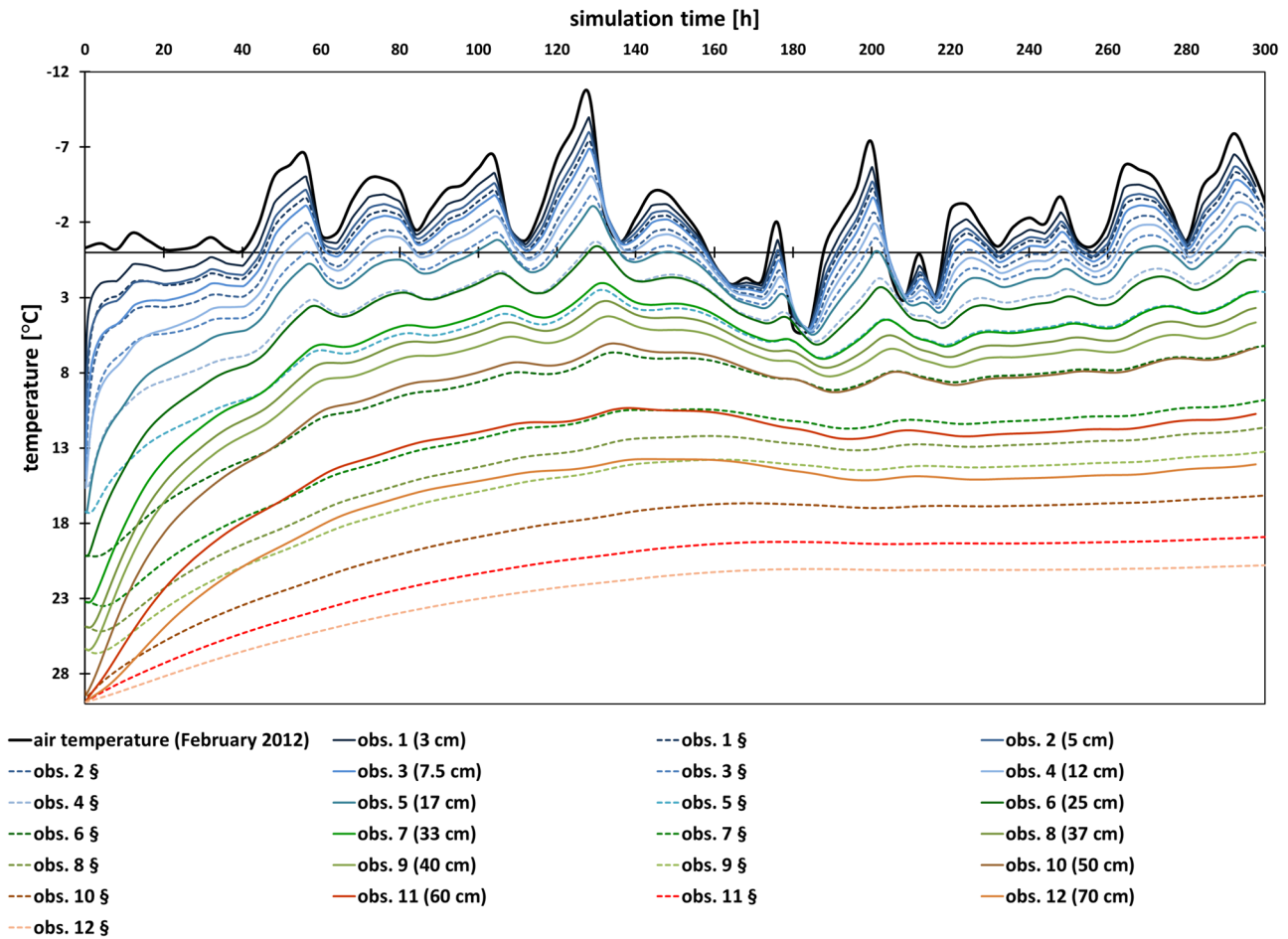- Very low porosity and very low hydraulic conductivity, due to the high state of compaction.

Fig. 7 Soil temperatures over time provided by the model in scenario B, at different distances from the upper boundary (obs. points 2 to 10 are located in the CC layer, while obs. points 11 and 12 are in the drainage layer below). For each location, the temperatures obtained by considering (solid line) or not considering (dotted line) the change in TC and heat capacity with freezing are shown. The black line represents the air temperature imposed at the upper boundary. The red vertical line indicates the time step (125 h) to which Fig. 6b, c refer

Conversely, the drainage and regularization layers are characterized by a very low thermal conductivity (0.3 ÷ 0.4 Wm^{-1} K^{-1}), due to the homogeneous clasts size, high porosity, and near-dry conditions of this layer.

Comparison between Fig. 6b, c, both for scenario B, provides a comparison of the temperature distribution at the time of the lowest air temperature (the same time step indicated by the red line in Fig. 7). In Fig. 6b, the specific plug-in that accounts for the change in thermal properties consequent to the freezing process and the latent heat release was applied, while Fig. 6c shows data obtained without the plug-in. The temperature pattern resulting from the model outputs is significantly different; when the freezing process is not properly accounted for, the frost front penetrates only 9 cm from the upper boundary (as depicted in Fig. 6c) and the thermal gradient is more constrained in the CC layer.

Figure 7 represents the temperature evolution over time provided by the model for scenario B at the most significant observation points located at increasing depths from the upper boundary (obs. points 2 to 10 are located in the CC layer, while obs. points 11 and 12 are located in the underlying drainage layer). For each point, the temperatures obtained considering the change in thermal properties due to the frozen condition (represented by solid lines) are directly compared to those obtained without (dotted lines). The direct comparison highlights that as soon as the soil freezing occurs, the increased TC and the lower heat capacity boost the penetration of the frost front, again emphasizing the importance of properly considering the freezing process and their effects on the thermal behavior of the soil.

It is important to note that the thickness of the CC barrier here is equal to 50 cm, as requested by local regulations. Considering the model outputs on the frost front penetration in scenario B, it appears that, under the studied conditions, about one-third (17 cm) of the top CC layer is subject to freezing. In fact, considering the change in thermal behavior,

the frost front penetrates quite rapidly in depth, boosted by (I) the changes in the thermal properties of the already frozen band, since in frozen conditions, the TC increases significantly (+80%) and the heat capacity decreases (-25%), and (II) some vertical migration of water (as far as allowed by the low hydraulic conductivity), which occurs along the thermal gradient from higher temperature areas towards lower temperature areas (Benson and Othman 1993; Henry 1988).

As reported in the Introduction, the literature widely agrees that the hydraulic conductivity of compacted clays is significantly affected by temperature variations, particularly by FT cycles, as demonstrated by previous experimental evidence and in situ measurements (Othman et al. 1994; Albrecht and Benson 2001; Sterpi 2015; Dalla Santa et al. 2020a). Considering the modeling results obtained in the considered study case, combined with data on the variation of hydraulic conductivity due to FT cycles acquired from recent experimental tests reported in Dalla Santa et al. (2020a), it is possible to estimate the variation of hydraulic conductivity of the entire CC barrier. Applying the permeability value of sample B reported in Dalla Santa et al. (2020a), the impermeable capacity of the entire CC layer increases from $k = 2.9*10^{-8}$ m/s (immediately after compaction) to $k = 4.3*10^{-8}$ m/s (with 17 cm of frost front penetration). Thus, in this case, the overall hydraulic conductivity of the CC layer increases by 50%, but, as already observed by Benson and Othman (1993) from in situ measurements, this does not exceed the values required by regulations.

Nevertheless, since FT cycles can degrade the impervious capacity of the CC barrier, the CC barrier of the upper landfill cover should not be left without the top protective layer of natural soil during colder months, when subzero air temperatures occur and, therefore, freeze–thaw cycles may occur in the upper part of the barrier. In fact, changes in the internal structure of the clay caused by freezing processes are irreversible, and the previous hydraulic conductivity cannot be restored; only cohesive materials with high plasticity indexes (PI > 24%) and high w_{opt} seem to have a partial self-healing capacity (Aldaeef and Rayhani 2015; Dalla Santa et al. 2020a).

Finally, it should be noted that the case study is located in the Po Valley in Northern Italy and is exposed to a temperate climate; therefore, the situation could be more serious in colder climates, with greater penetration of the frost front, and consequently more intense weakening of the effectiveness of the entire CC barrier due to freezing. Further research could consider the effects of different climates leading to different temperature boundary conditions.

This research highlights the importance of considering the change in thermal behavior due to phase change, in the evaluation of soil volume involved in the development of temperature pattern, and, in particular, in the evaluation of

frost front development. In addition, a first set of experimental values of thermal conductivity and volumetric heat capacity of frozen silty clay is provided. These results should also be considered to address issues in other fields of application, such as, for example, the evaluation of the volume of soil involved in permafrost thawing due to climate change, which can result in distributed differential settlements in linear communication routes such as roads or railways, or in building foundations, and can damage underground utilities. Another area of application may be the assessment of the volume of soil involved in seasonal freeze/thaw at high altitude locations, either in the case of loose materials, fractured rock masses, or rock glaciers, where phase change may cause loss of strength and cohesion and eventually result in local slope instability and landslides. The same approach also need to be considered in technical engineering applications, such as artificial ground freezing to support tunnel excavations, when evaluating freeze-induced annular protection widening, or when evaluating the volume of material involved in artificial deicing when applied to roads, viaducts, bridges, or inclined ramps.

Conclusions

In landfills, the effectiveness of isolating waste disposal to limit its impact on the environment and public health relies on the impermeability of the properly compacted clay layer. However, the hydraulic conductivity of the CC layer can be modified by thermal alteration and particularly by FT cycles.

The direct measurements and the modeling here presented yielded the following results:

1. Experimental values of the thermal properties of the materials sampled from the layers constituting the landfill cover (gravelly drainage layer, CC barrier, and the two geosynthetics) under different conditions of water content and temperature were provided. These values are the first important result of this research, because thermal properties of frozen soils are rare in literature, and they can be useful in other applications.

2. The obtained thermal parameters were applied to a 2D FE model, in order to evaluate the temperature distributions within the landfill cover in the temporary configuration (without the top protective soil layer) exposed to air temperature fluctuations and heat generated by the waste mass degradation. The outputs indicate that, in scenario A, almost the entire CC barrier is exposed to temperatures above 30° that can lead to drying processes. In scenario B, the outputs reveal that the frost front can penetrate significantly (up to 17 cm) in the CC barrier from the upper edge (Fig. 6b).

3. In the considered study case, the entire CC barrier has a thickness of 50 cm (as required by Italian regulations),

and the model outputs estimate that about one-third of the CC barrier is affected by penetration of the freezing front, which is favored by the enhanced thermal behavior of the CC layer under frozen conditions. As a result, the thickness of the CC layer that is in fact characterized by hydraulic conductivity achieved through the initial compaction is reduced, and, therefore, the effectiveness of the whole barrier may deteriorate.

4. In the study case, the final overall hydraulic conductivity of the CC layer results 50% higher than before, although it does not exceed the standard values required, but the situation may be more serious in colder climates, with greater penetration of the frost front, and consequently a more intense weakening of the effectiveness of the whole CC barrier due to freezing.

To conclude, in the practical application of landfill engineering, it is important to consider that, if the top barrier of a landfill is kept in a temporary configuration without the protective layers, its effectiveness in insulating disposed waste could be damaged throughout the expected life of the landfill, depending on the temperature changes experienced. Even if immediately after installation the CC layer material meets regulatory requirements in terms of hydraulic conductivity, the effective impervious capacity of the entire barrier could be significantly lower. For this reason, the final protective layers should be laid as soon as possible and, in particular, before subzero air temperatures occur.

References

Albrecht B, Benson C (2001) Effect of desiccation on compacted natural clays. J Geotech Geoenviron 127(1):67–76

Aldaeef AA, Rayhani MT (2014) Hydraulic performance of Compacted Clay Liners (CCLs) under combined temperature and leachate exposures. Waste Manage 34(12):2548–2560. https://doi.org/10.1016/j.wasman.2014.08.007

Aldaeef AA, Rayhani MT (2015) Hydraulic performance of compacted clay liners under simulated daily thermal cycles. J Environ Manage 162:171–178. https://doi.org/10.1016/j.jenvman.2015.07.036

Applied Precision (2013) ISOMET 2114 Thermal properties analyzer. User's Guide

Aziz HA, Yik WC, Ramli H, Amr SSA (2016) Investigations on the hydraulic conductivity and physical properties of silt and sludge as potential landfill capping material. International Journal of GEOMATE 10(22):1989–1993

Benson CH, Albright W, Fratta D, Tinjum J, Kucukkirca E, Lee S, Scalia J, Schlicht P, Wang X (2011) Engineered covers for waste containment: changes in engineering properties & implications for long-term performance assessment. NUREG/CR-7028 Office of Research U.S. Nuclear Regulatory Commission, Washington

Benson CH, Othman M (1993) Hydraulic conductivity of compacted clay frozen and thawed in situ. J Geotech Eng 119(2):276–294

Casasso A, Sethi R (2015) Modelling thermal recycling occurring in groundwater heat pumps (GWHPs). Renewable Energy 77:86–93. https://doi.org/10.1016/j.renene.2014.12.003

Chamberlain EJ, Gow AJ (1979) Effects of freezing and thawing on permeability and structure of soils. Eng Geol 13(1):73–92

Chegenizadeh A, Keramatikerman M, Dalla Santa G, Nikraz H (2018) Influence of recycled tyre amendment on the mechanical behaviour of soil-bentonite cut-off walls. J Clean Prod 177:507–515. https://doi.org/10.1016/j.jclepro.2017.12.268

Chiemchaisri C, Chiemchaisri W, Chittanukul K, Soontornlerdwanich W, Tanthachoon N (2010) Effect of leachate irrigation on methane oxidation in tropical landfill cover soil. J Mater Cycles Waste Manage 12(2):161–168

Cultrera M, Boaga J, Di Sipio E, Dalla Santa G, De Seta M, Galgaro A (2018) Modelling an induced thermal plume with data from electrical resistivity tomography and distributed temperature sensing: a case study in northeast Italy. Hydrogeol J 26(3):837–851. https://doi.org/10.1007/s10040-017-1700-3

Dalla Santa G, Cola S, Tateo F, Galgaro A (2016) Modified compressibility of cohesive sediments induced by thermal anomalies due to a borehole heat exchanger. Eng Geol 202:143–152. https://doi.org/10.1016/j.enggeo.2016.01.011

Dalla Santa G, Peron F, Galgaro A, Cultrera M, Bertermann D, Mueller J, Bernardi A (2017) Laboratory measurements of gravel thermal conductivity: an update methodological approach. Energy Procedia 125:671–677. https://doi.org/10.1016/j.egypro.2017.08.287

Dalla Santa G, Cola S, Secco M, Tateo F, Sassi R, Galgaro A (2019a) Multiscale analysis of freeze-thaw effects induced by ground heat exchangers on permeability of silty-clays. Geotechnique 69(2):95–105. https://doi.org/10.1680/jgeot.16.p.313

Dalla Santa G, Farina Z, Anbergen H, Rühaak W, Galgaro A (2019b) Relevance of computing freeze-thaw effects for borehole heat exchanger modelling: a comparative case study. Geothermics 79:164–175. https://doi.org/10.1016/j.geothermics.2019.02.001

Dalla Santa G, Cola S, Tateo F, Galgaro A (2020a) Hydraulic conductivity changes in compacted clayey barriers due to temperature variations in landfill top covers. B Eng Geol Environ 79(6):2893–2905. https://doi.org/10.1007/s10064-020-01726-w

Dalla Santa G, Galgaro A, Sassi R, Cultrera M, Scotton P, Mueller J, Bertermann D, Mendrinos D, Pasquali R, Perego R, Pera S, Di Sipio E, Cassiani G, De Carli M, Bernardi A (2020b) An updated ground thermal properties database for GSHP applications. Geothermics 85:101758. https://doi.org/10.1016/j.geothermics.2019.101758

DHI (2017a) Feflow, Finite Element Subsurface Flow & Transport Simulation System - Reference Manual. DHI, Berlin, German.

DHI (2017b) PiFreeze. A freeze/thaw plug-in for FEFLOW - user guide. DHI, Berlin, German.

Diersch H-JG (2005) Discrete feature modeling of flow, mass and heat transport processes by using FEFLOW. In: Wasy G (ed) Wasy Software. Finite Element Subsurface Flow & Transport Simulation System - White Papers, Berlin, p 46

Diersch H-JG (2014) FEFLOW-finite element modeling of flow, mass and heat transport in porous and fractured media. Springer-Verlag.

Dogan A, Motz HL (2005a) Saturated-unsaturated 3d groundwater model. I: Development. J Hydrol Eng 10:492–504. https://doi.org/10.1061/(ASCE)1084-0699(2005)10:6(492)

Dogan A, Motz HL (2005b) Saturated-unsaturated 3d groundwater model. II: Verification and Application. J Hydrol Eng 10:505–515. https://doi.org/10.1061/(ASCE)1084-0699(2005)10:6(505)

El-Fadel M, Khoury R (2000) Modeling settlement in MSW landfills: a critical review. Crit Rev Env Sci Technol 30(3):327–361

Faitli J, Magyar T, Erdélyi A, Murányi A (2015) Characterization of thermal properties of municipal solid waste landfills. Waste Manag 36:213–221. https://doi.org/10.1016/j.wasman.2014.10.028

Farouki OT (1981) Thermal properties of soils. DTIC Document.

Fricke BA, Misra A, Becker BR, Stewart WE (1992) Soil thermal conductivity: effects of saturation and dry density. In: Thermal Performance of the Exterior Envelopes of Whole Buildings V International Conference, Clearwater Beach, Florida, USA.

Galgaro A, Dalla Santa G, Cola S, Cultrera M, De Carli M, Conforti F, Scotton P, Viesi D, Fauri M (2020) Underground warehouses for food storage in the Dolomites (Eastern Alps – Italy) and energy efficiency. Tunn Undergr Sp Tech 102:103411. https://doi.org/10.1016/j.tust.2020.103411

Hanson JL, Liu WL, Yesiller N (2008) Analytical and numerical methodology for modeling temperatures in landfills. In: GeoCongress 2008: Geotechnics of Waste Management and Remediation pp 24–31

Hanson JL, Yeşiller N, Oettle NK (2009) Spatial and temporal temperature distributions in municipal solid waste landfills. J Environ Eng 136:804–814

Hanson JL, Yeşiller N, Onnen MT, Liu W-L, Oettle NK, Marinos JA (2013) Development of numerical model for predicting heat generation and temperatures in MSW landfills. Waste Manag 33:1993–2000. https://doi.org/10.1016/j.wasman.2013.04.003

Henry K (1988) Chemical aspects of soil freezing. Hanover, NH: U.S. Army Corps of Engineers, Cold Regions Research and Engineering Lab (No. CRREL-88-17)

Herrmann I, Svensson M, Ecke H, Kumpiene J, Maurice C, Andreas L, Lagerkvist A (2009) Hydraulic conductivity of fly ash–sewage sludge mixes for use in landfill cover liners. Water Res 43(14):3541–3547. https://doi.org/10.1016/j.watres.2009.04.052

Jones BW (1988) Thermal conductivity probe: development of method and application to a coarse granular medium. J Phys E: Sci Instrum 21(9):832

Kim WH, Daniel DE (1992) Effects of freezing on hydraulic conductivity of compacted clay. J Geotech Eng 118(7):1083–1097. https://doi.org/10.1061/(ASCE)0733-9410(1992)118:7(1083)

Kömle NI, Hütter ES, Feng WJ (2010) Thermal conductivity measurements of coarse-grained gravel materials using a hollow cylindrical sensor. Acta Geotech 5(4):211223

Konrad J-M (1989) Physical processes during freeze-thaw cycles in clayey silts. Cold Reg Sci Technol 16:291–303

Moo-Young HK, Zimmie TF (1996) Geotechnical properties of paper mill sludges for use in landfill covers. J Geotech Eng 122(9):768–775

Morris DV, Woods CE (1990) Settlement and engineering considerations in landfill and final cover design. In: Geotechnics of waste fills—theory and practice. ASTM International, West Conshohocken

Murray EJ, Rix DW, Humphrey RD (1996) Evaluation of clays as linings to landfill. Geol Soc Lond 11:251–258. https://doi.org/10.1144/GSL.ENG.1996.011.01.34

Nikolaev IV, Leong WH, Rosen MA (2013) Experimental investigation of soil thermal conductivity over a wide temperature range. Int J Thermophys 34:1110–1129. https://doi.org/10.1007/s10765-013-1456-5

Othman MA, Benson CH, Chamberlain EJ, Zimmie TF (1994) Laboratory testing to evaluate changes in hydraulic conductivity of compacted clays caused by freeze-thaw: state-of-the-art. In: Hydraulic Conductivity and Waste Contaminant Transport in Soil, American Society for Testing and Materials Standard International

Perego R, Viesi D, Pera S, Dalla Santa G, Cultrera M, Visintainer P, Galgaro A (2020) Revision of hydrothermal constraints for the installation of closed-loop shallow geothermal systems through underground investigation, monitoring and modeling. Renewable Energy 153:1378–1395. https://doi.org/10.1016/j.renene.2020.02.068

Qi J, Ma W, Song C (2008) Influence of freeze–thaw on engineering properties of a silty soil. Cold Reg Sci Technol 53:397–404. https://doi.org/10.1016/j.coldregions.2007.05.010

Rowe RK (2005) Long-term performance of contaminant barrier systems. Geotechnique 55:631–678

Scaringi G, Loche M (2022) A thermo-hydro-mechanical approach to soil slope stability under climate change. Geomorphology 401:108108. https://doi.org/10.1016/j.geomorph.2022.108108

Schön JH (2015) Physical properties of rocks: fundamentals and principles of petrophysics (Vol. 65) Elsevier

Singh RM, Bouazza A (2013) Thermal conductivity of geosynthetics. Geotext Geomembr 39:1–8. https://doi.org/10.1016/j.geotexmem.2013.06.002

Sterpi D (2015) Effect of freeze–thaw cycles on the hydraulic conductivity of a compacted clayey silt and influence of the compaction energy. Soils Found 55:1326–1332. https://doi.org/10.1016/j.sandf.2015.09.030

Tarnawski VR, Gori F, Wagner B, Buchan GD (2000) Modelling approaches to predicting thermal conductivity of soils at high temperatures. Int J Energy Res 24:403–423

Victoria EPA (2015) Siting, design, operation and rehabilitation of landfills. Environmental Protection Authority (EPA) Victoria, EPA Victoria, Carlton, available at http://www.epa.vic.gov.au/~/media/Publications/788, 203

Yeşiller N, Hanson JL, Oettle NK, Liu W-L (2008) Thermal analysis of cover systems in municipal solid waste landfills. J Geotech Geoenvironmental Eng 134:1655–1664